UNCLASSIFIED

SECURITY CLASSIFICATION OF THIS PAGE (When Data Entered)

REPORT DOCUMENTATION PAGE

READ INSTRUCTIONS BEFORE COMPLETING FORM

1. REPORT NUMBER: SAM-TR-77-33	2. GOVT ACCESSION NO.
3. RECIPIENT'S CATALOG NUMBER: Rept.	
4. TITLE (and Subtitle): TRANSFER FUNCTIONS FOR EYE-LEVEL BLOOD PRESSURE DURING +G STRESS.	5. TYPE OF REPORT & PERIOD COVERED: Final June 74-June 77
6. PERFORMING ORG. REPORT NUMBER	
7. AUTHOR(s): Kent F. Gillingham, James M. Freeman and Richard C. McNee	8. CONTRACT OR GRANT NUMBER(s): 79[illegible], 17[illegible]
9. PERFORMING ORGANIZATION NAME AND ADDRESS: USAF School of Aerospace Medicine, Brooks AFB, TX 78235	10. PROGRAM ELEMENT, PROJECT, TASK AREA & WORK UNIT NUMBERS: 7930-03-49, 7930-13-09
11. CONTROLLING OFFICE NAME AND ADDRESS: USAF School of Aerospace Medicine, Brooks AFB, TX 78235	12. REPORT DATE: 15 June 1977
	13. NUMBER OF PAGES: 11 p.
14. MONITORING AGENCY NAME & ADDRESS (if different from Controlling Office)	15. SECURITY CLASS (of this report): Unclassified
	15a. DECLASSIFICATION DOWNGRADING SCHEDULE

16. DISTRIBUTION STATEMENT (of this Report)

Approved for public release; distribution unlimited.

DDC RECEIVED NOV 21 1977 B

17. DISTRIBUTION STATEMENT (of the abstract entered in Block 20, if different from Report)

18. SUPPLEMENTARY NOTES

To be published in "Aviation, Space, and Environmental Medicine."

19. KEY WORDS (Continue on reverse side if necessary and identify by block number)

acceleration	blood pressure
G stress	carotid sinus
baroreceptors	stress physiology

(+Gz)

20. ABSTRACT (Continue on reverse side if necessary and identify by block number)

A description of the eye-level blood-pressure response to +Gz stress in relaxed humans was obtained as an empirical, ensemble-average, G-to-blood-pressure transfer function based on 3 subjects' responses to a total of 23 simulated aerial combat maneuvering runs on the USAFSAM Human Centrifuge. Three different analytic transfer functions were fitted to the empirical function for frequencies from 5 to 200 mHz, and predictive performance of the empirical and 3 analytic functions was examined. The double-zero, double-pole

DD FORM 1 JAN 73 1473 EDITION OF 1 NOV 65 IS OBSOLETE

317 080

UNCLASSIFIED

SECURITY CLASSIFICATION OF THIS PAGE (When Data Entered)

BEST AVAILABLE COPY

AD A046738

DDC FILE COPY

mathematical model most closely fit the empirical transfer function and displayed reasonable predictive ability.

Transfer Functions for Eye-Level Blood Pressure During $+G_z$ Stress

KENT K. GILLINGHAM, JAMES J. FREEMAN, and RICHARD C. MCNEE

Biodynamics and Design and Analysis Branches, USAF School of Aerospace Medicine, Brooks Air Force Base, Texas 78235

GILLINGHAM, K. K., J. J. FREEMAN, and R. C. MCNEE. *Transfer functions for eye-level blood pressure during $+G_z$ stress.* Aviat. Space Environ. Med. 48(11):1026-1034, 1977.

A description of the eye-level blood-pressure response to $+G_z$ stress in relaxed humans was obtained as an empirical, ensemble-average, G-to-blood-pressure transfer function based on three subjects' responses to a total of 23 simulated aerial combat maneuvering runs on the USAFSAM human centrifuge. Three different analytic transfer functions were fitted to the empirical function for frequencies from 5 to 200 mHz, and predictive performance of the empirical and three analytic functions was examined. The double-zero, double-pole mathematical model most closely fit the empirical transfer function and displayed reasonable predictive ability.

A CONCISE DESCRIPTION of the human eye-level arterial blood-pressure response to $+G_z$ stress is lacking. It is well established (2) that a hydrostatic column effect acts to reduce blood pressure at eye level below that at heart level: the amount of this reduction would be equal to $d \cdot a \cdot h$, where d is the density of blood, a is the ambient acceleratory field, and h is the vertical heart-to-eye distance (approximately 30 cm), if the cardiovascular system were to respond as a passive, rigid-walled system. To such a system, the change in eye-level blood pressure during G stress could be described simply as -3.0×10^4 dynes/cm^2/G, or about -22 mm Hg/G. Because the arterial system is a distensible hydraulic column, as pointed out by Lawton, *et al.* (9), and the cardiovascular (baroceptor) reflexes serve to counter G-stress-induced reductions in eye-level arterial pressure (3,6,11), the description of blood pressure as a function of G load and time is considerably complicated. Mathematical models of the relation between G load and blood pressure have been based on animal experiments (5,15) and on deconvolution of scarce, published human blood-pressure response curves (12), but adequate data upon which to base a useful model of human blood-pressure response to G stress have hitherto not been available. An efficient method for obtaining a description of human arterial oxygen saturation during $+G_z$ stress was recently reported (4): ratios of Fourier transforms of output oxygen saturation to input G stress provided frequency response curves—i.e., transfer functions—describing the general mathematical relationship between those variables. Despite the fact that the biological system under test was brashly assumed to be linear and stationary, surprisingly consistent descriptions with reasonable predictive ability were obtained. By employing a method of analysis similar to that reported, we sought a workable transfer function for the human eye-level blood-pressure response to $+G_z$ stress.

MATERIALS AND METHODS

Three, healthy, male, 24, 25, and 26 year-old volunteer members of the USAFSAM Acceleration Stress Panel provided the data reported herein. The left radial artery of each was cannulated with a 5-cm Medicut® 18-gauge catheter, and an adequate length of saline-filled, noncompliant, 15-gauge Teflon® tubing connected the arterial catheter to a Statham P37 pressure transducer mounted on a Velcro® headband at eye level. A three-way stopcock, inserted between the arterial catheter and the tubing, allowed periodic flushing of the catheter with heparinized saline. The output voltage of the pressure transducer, corresponding to instantaneous eye-level blood pressure, was recorded on magnetic tape.

Subjects were exposed in a seated (13° seatback angle), relaxed condition—without benefit of anti-G suit or straining maneuver—to three different categories of G stress on the centrifuge: 1) gradual-onset runs (GORs), in which the G load increased linearly with time at the rate of 0.067 G/s; 2) rapid-onset runs (RORs), in which the G load rose at about 1.0 G/s to a predetermined level and remained at that level for either 15 s or 1 min; and 3) simulated aerial combat maneuvers (SACMs), in which G loads were applied in a varying manner over a 100-s period. The SACM G profiles were of eight different shapes, each profile having been produced by a random function generator with bandwidth set to match the capabilities of the

The research reported in this paper was conducted by personnel of the Crew Technology and Biometrics Divisions, USAF School of Aerospace Medicine.

J. J. Freeman is a USAF-ASEE Summer Faculty Research Program Participant, 1976

The voluntary informed consent of the subjects used in this research was obtained in accordance with AFR 80-33.

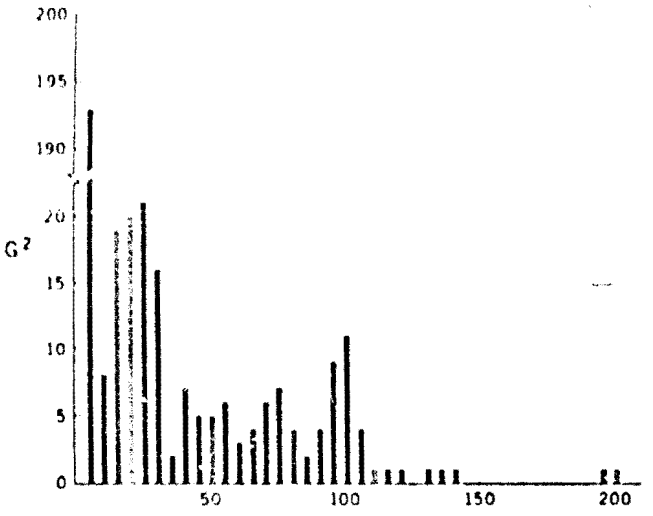

Fig. 1. Power spectrum of #8 SACM G profile as run on USAFSAM Human Centrifuge. 95% of power is below 95 mHz, 99% below 110 mHz. Other G profiles exhibit similar bandwidths.

USAFSAM Human Centrifuge (Fig. 1); some profiles were augmented or clipped, as necessary, to challenge the subjects' visual functioning without rendering them unconscious.

Subjects were instructed to relax completely during all test runs, and to release a hand-held enabling switch—thus terminating the run—whenever they experienced the visual endpoint, which consisted of total loss of peripheral vision plus significant deterioration of central vision. Each subject was exposed to the following: one GOR to visual endpoint; three to five 15-s RORs, the final one eliciting the visual endpoint; at least one 60-s ROR; and four to 11 SACMs, several of which elicited the visual endpoint in two of the three subjects. The one subject who sustained only four SACMs terminated the experiment early because of motion sickness.

Discrete, finite Fourier transforms of 200-s records of input (G stress) and output (eye-level arterial blood pressure) were obtained with a Hewlett-Packard 5451B Fourier Analyzer. To convert the instantaneous blood-pressure signal to mean blood pressure, and to prevent spectral aliasing of the transformed data, both input and output signals were low-pass filtered with a 0.5-Hz, 48-dB/octave Butterworth filter. The paired input and output waveforms were sampled 256 times during the 200-s analysis period, T; i.e., $\Delta t = 0.78$ s. The spectra obtained, therefore, had a maximum frequency of 0.64 Hz [$f_{max} < (2\ \Delta t)^{-1}$] and a frequency resolution of 5.0 mHz ($\Delta f = 1/T$). As the transient time-domain signals of interest began and ended well within the 200-s analysis period, the rectangular time window used was optimum for the present application.

The transfer function, H(f), between a G-stress input, i(t), and blood-pressure output, o(t), was obtained by dividing the Fourier transform of the output, O(f), by that of the input, I(f); i.e.,

$$H(f) = \frac{O(f)}{I(f)} \qquad \text{(Eq. 1)}$$

By ensemble averaging transfer functions obtained from single input-output pairs, a *mean* transfer function, $\bar{H}(f)$, derived from all pertinent data in a data set (e.g., one type of G-stress profile) was readily obtained. Spectral inconsistencies (noise) were appreciably reduced by this process. Mean responses to specific input functions were obtained by averaging the transfer functions generated by that input and the responses to it, and transforming to the time domain the product of the average transfer function and the Fourier transform of the input; i.e.,

$$\bar{O}(f) = \bar{H}(f)\ I(f) \qquad \text{(Eq. 2)}$$

where $\bar{O}(f)$ is the Fourier transform of the mean output, $\bar{o}(t)$.

Multiplying a transfer function by the Fourier transform of a particular input of interest provided the predicted response to that input, based on the given transfer function. In other words,

$$O'(f) = H(f)\ I'(f) \qquad \text{(Eq. 3)}$$

where I'(f) is the Fourier transform of the input of interest, i'(t), and O'(f) is the Fourier transform of the predicted response, o'(t).

Because the power spectra of the SACMs extended to relatively high frequencies without regular spectrum nulls, the mean transfer function obtained by ensemble averaging the transfer functions from the 23 completed and aborted SACMs was examined most thoroughly and with the greatest expectations. This averaging process gave each of the 23 SACM runs equal weight in the mean transfer function. The alternative method—averaging each subject's SACM-generated transfer functions and then averaging the three subjects' mean transfer functions—was also accomplished, but this process theoretically gave undue weight to the noise associated with the responses of the subject exposed to only four SACMs. Each subject's individual transfer functions, as well as the three subjects' mean transfer functions, were sufficiently similar that the two methods of averaging the SACM-generated transfer functions yielded nearly identical overall mean transfer functions.

Having obtained the empirical transfer function related eye-level blood pressure to $+G_z$ stress from the ensemble average of the SACM-generated transfer functions, we elected to find several mathematically well-behaved substitutes for the empirical transfer function. The analytic transfer functions sought were of three forms: 1) single-zero, double-pole; 2) double-zero, double-pole; and 3) single-zero, double-pole with a delayer. Parameter estimates were obtained for each analytic form by minimizing the weighted sum of the squared error of the fit of real and imaginary terms of the analytic form to the first 40 frequencies of the empirical transfer function. The weight used at each frequency was inversely proportional to the variance of the data comprising the empirical function at that fre-

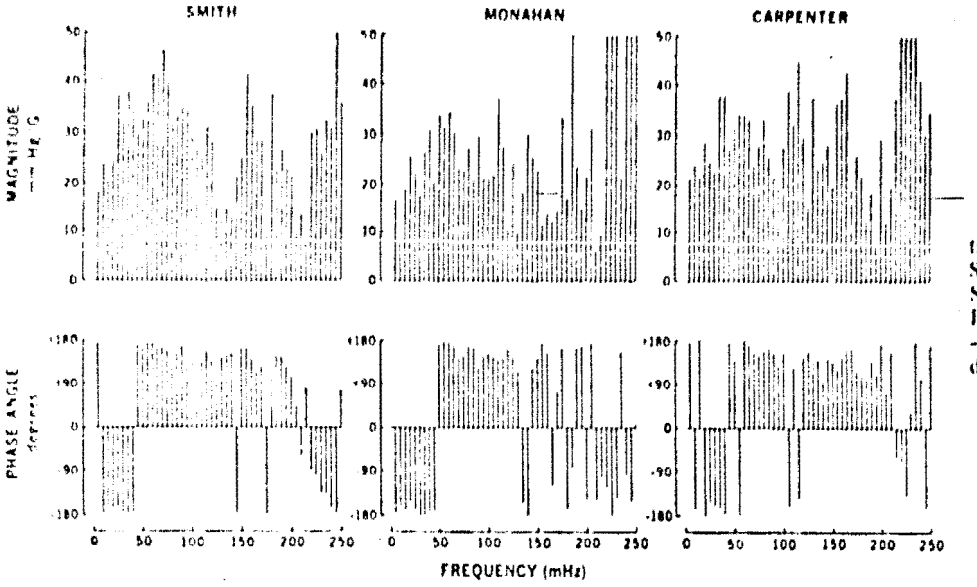

Fig. 2. Mean G-to-blood-pressure transfer functions derived from SACM G-stress runs of subjects Smith, Monahan, and Carpenter. First 50 frequencies—5 to 250 mHz—displayed at 5-mHz Δf. Unedited data.

quency. Marquardt's algorithm, combining the Taylor series expansion and negative gradient methods, was used in the computations.

Finally, predictions of eye-level blood-pressure responses to GOR, ROR, and SACM G stresses, based on the empirical and various analytic transfer functions, were compared with the mean actual responses to the same G-stress inputs. Such comparisons gave visual evidence of the relative merits of each of the transfer functions being studied.

RESULTS

Each subject's mean G-to-blood-pressure transfer function obtained from SACM G-stress runs is shown in linear-scale, polar form, in Fig. 2. Note the similar frequency characteristics; namely, the apparent resonance peak at approximately 60 mHz; the tendency toward −180° phase at low frequencies, a phase crossover to +180° at about 40 mHz, and a progressive decrease in phase angle at higher frequencies. The mean transfer function for all 23 SACM G-stress runs, i.e.,

$$\bar{H}(f) = \frac{1}{23} \sum_{i=1}^{23} H_i(f)$$

is presented in Fig. 3. The frequency characteristics that were seen in the subjects' mean transfer functions are again evident, as is the improvement in the signal-to-noise ratio resulting from the additional averaging. In this overall mean transfer function, the resonance peak is seen to be at 60 mHz, the phase crossover occurs at between 40 and 45 mHz, and a local maximum in the phase characteristic is noticeable at 25 mHz. In addition, a 4-dB/octave decline in magnitude can be estimated for frequencies beyond the resonance. Above 200 mHz no useful information appears in the frequency response curve, as input power associated with the SACM G-force profiles was virtually nonexistent above this frequency. The first 40 terms of the 23-run mean transfer function are given in Table I.

The relatively smooth contours of the above empirically determined transfer function enticed us to search for analytic functions which could effectively duplicate

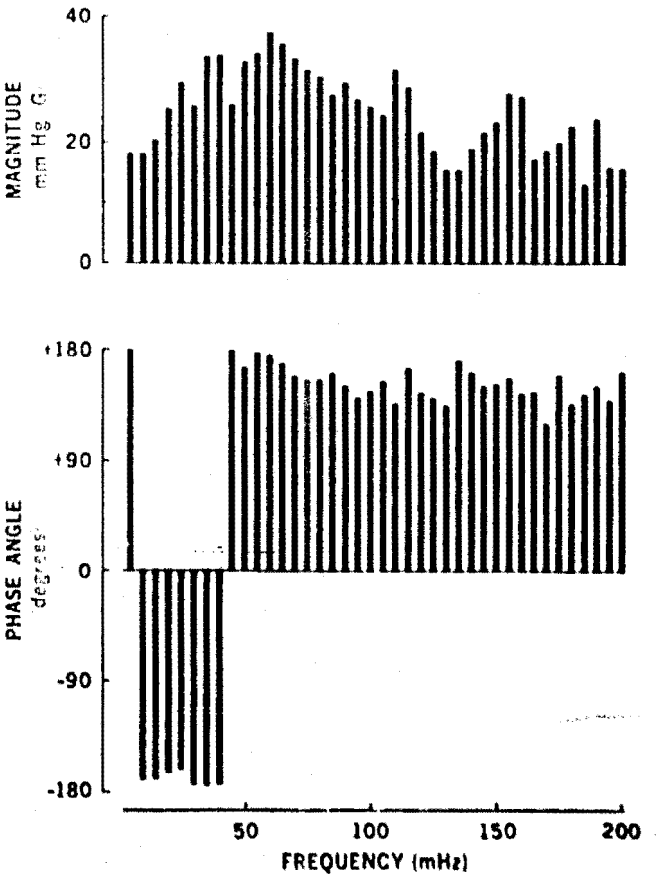

Fig. 3. Mean transfer function for 23 SACM G-stress runs. Each run was given equal weight in the averaging. Four aberrant points were edited prior to summing.

TABLE I. EMPIRICAL G-TO-BLOOD-PRESSURE TRANSFER FUNCTION: MEAN OF 23 SACM RUNS

Frequency (mHz)	Magnitude (mm Hg/G)	Phase (degrees)
5	18.2	178.7
10	18.2	—169.3
15	20.3	—168.6
20	25.1	—163.0
25	29.4	—161.1
30	25.8	—174.2
35	33.6	—174.9
40	33.8	—174.4
45	25.8	178.0
50	32.8	163.9
55	34.1	176.0
60	37.4	174.1
65	35.6	167.8
70	33.1	156.4
75	31.3	154.2
80	30.1	154.1
85	27.4	159.3
90	29.3	149.0
95	26.7	139.2
100	25.6	145.1
105	24.2	152.0
110	31.3	135.0
115	28.5	163.7
120	21.5	143.4
125	18.7	138.9
130	15.4	133.1
135	15.3	170.3
140	18.9	159.9
145	21.4	149.3
150	23.1	151.3
155	27.6	155.3
160	27.1	143.2
165	17.2	144.5
170	18.7	118.9
175	20.0	156.8
180	22.6	134.9
185	12.9	142.3
190	23.8	149.3
195	16.0	138.1
200	15.6	160.7

the empirical one. First to be evaluated was a single-zero, double-pole transfer function:

$$H(s) = -16.2 \frac{1 + 12.0s}{1 + 6.74s + 7.11s^2} \quad \text{(Eq. 4)}$$

where s is the conventional complex frequency variable, $j2\pi f$. This transfer function, presented in linear-scale, polar form in Fig. 4, shows a resonance peak at 60 mHz, a local maximum in phase angle at 15 mHz, a phase crossover between 40 and 45 mHz, and high-frequency magnitude and phase-angle declines similar to those of the empirical transfer function.

The double-zero, double-pole transfer function,

$$H(s) = -18.3 \frac{1 + 7.18s + 4.39s^2}{1 + 3.99s + 7.93s^2} \quad \text{(Eq. 5)}$$

is shown in Fig. 5. Again, resonance is seen at 60 mHz, but the resonance peak is sharper than in the single-zero, double-pole transfer function. The local phase-angle maximum is seen at 25 mHz and the phase crossover occurs between 50 and 55 mHz. A continuing high-frequency decline in magnitude is not provided by this transfer function, although a decline comparable to that of the empirical transfer function is evident in the 60- to 200-mHz range. After the phase crossover, the phase angle falls and rises again. Such behavior is not necessarily incongruous with that of the phase characteristic of the empirical transfer function since, in the latter, noise may be obscuring a slight upward trend.

Finally, we fitted to the empirical transfer function an analytic function consisting of one zero, two poles, and an exponential term:

$$H(s) = -18.1 \frac{1 + 7.66s}{1 + 4.46s + 7.63s^2} e^{0.46s} \quad \text{(Eq. 6)}$$

The positive exponent, serving to augment the phase angle in proportion to frequency, implies anticipatory behavior of the function: our observation of occasional rises in blood pressure prior to onset of G stress prompted us to evaluate this type of transfer function. The fitted function (Fig. 6) displays the resonance peak, phase crossover, and other features of the empirical transfer function derived from the 23 SACM runs.

We noted with satisfaction that the steady-state char-

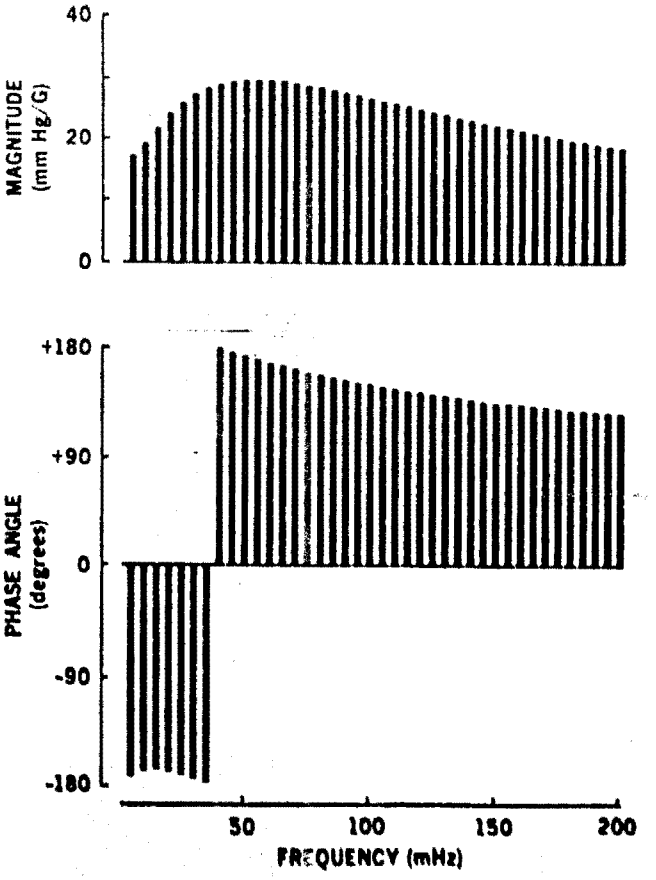

Fig. 4. Single-zero, double-pole transfer function fitted to empirical transfer function in Fig. 3. Parameters in text.

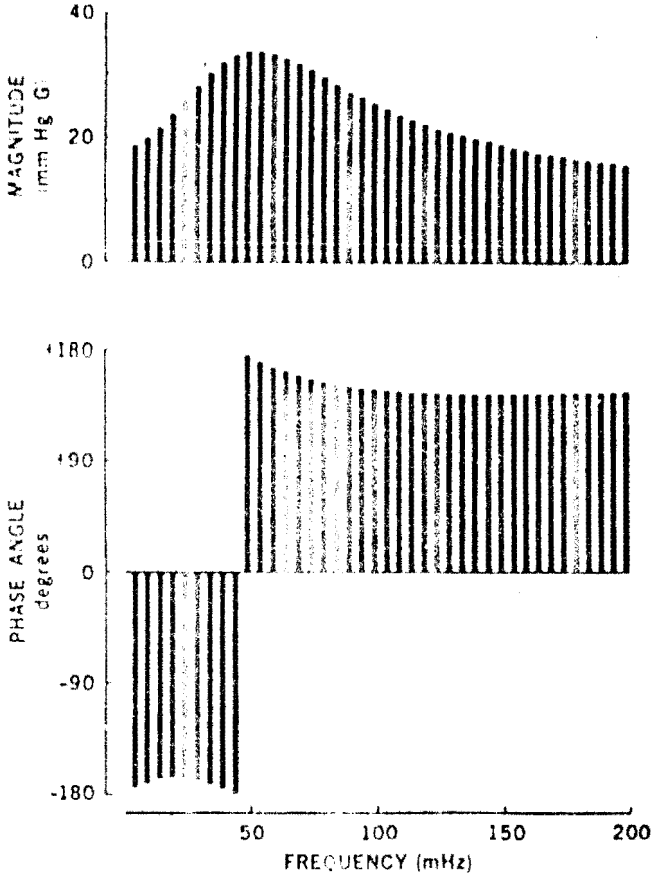

Fig. 5. Double-zero, double-pole transfer function fitted to empirical transfer function.

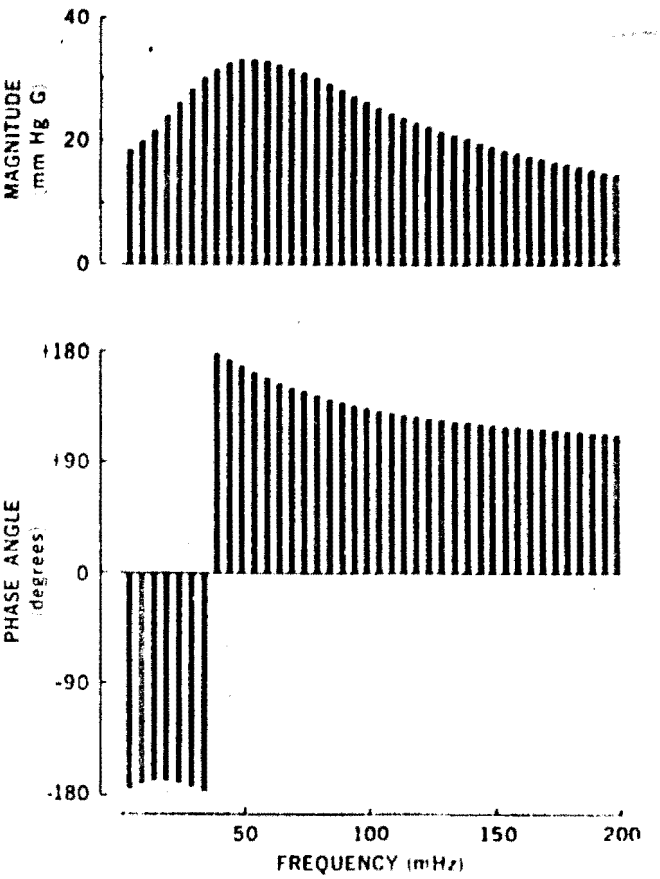

Fig. 6. Single-zero, double-pole, exponential transfer function fitted to empirical transfer function.

acteristics of the second two fitted analytic transfer functions came out to be −18.3 and −18.1—not too far from the theoretical −17.2 mm Hg/G discussed earlier.

By taking the inverse Fourier transform of the transfer function for a system, one obtains its impulse response, h(t), the time-domain response of the system to a forcing function of infinite amplitude and infinitesimal duration. The inverse transform of the complete empirical transfer function was too corrupted by high-frequency noise for a meaningful impulse response to be recognized, and inverse transforms of truncated versions of the empirical transfer function were somewhat distorted by truncation artifacts (Gibbs' phenomenon). The inverse Fourier transforms of the analytic transfer functions, however, appeared as reasonable impulse responses. Fig. 7 is the impulse response corresponding to the double-zero, double-pole transfer function; the inverse transforms of the other two analytic transfer functions were similar. The initial negative-going blood-pressure response—to the theoretical positive G force impulse applied at $t = 0$—is readily apparent, as is the zero-line crossing at 4.0 s and the subsequent rebound peak at 7.0 s. The high-frequency oscillation in the impulse response is an artifact resulting from the unavoidable truncation of the infinite analytic transfer functions.

Since the utility of a transfer function is determined not by how mathematically well behaved it is but by how well it predicts responses, we compared the predicted responses of the 23-run mean empirical and the three analytic transfer functions to the subjects' mean actual

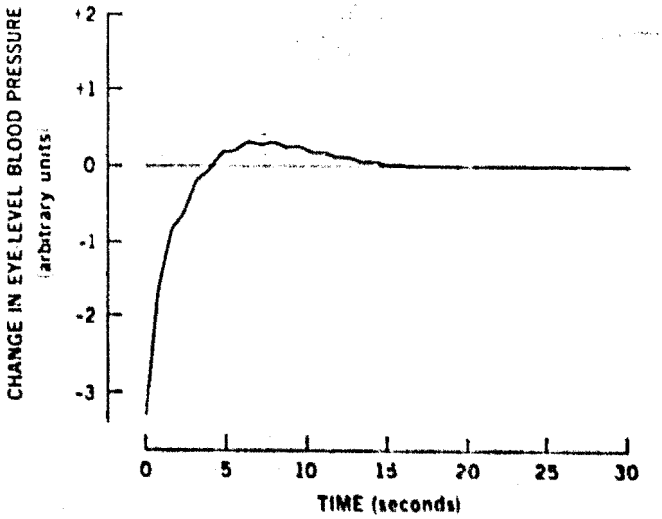

Fig. 7. Inverse Fourier transform (impulse response) of double-zero, double-pole transfer function. All 128 available frequencies—5 to 640 mHz—were used in computation.

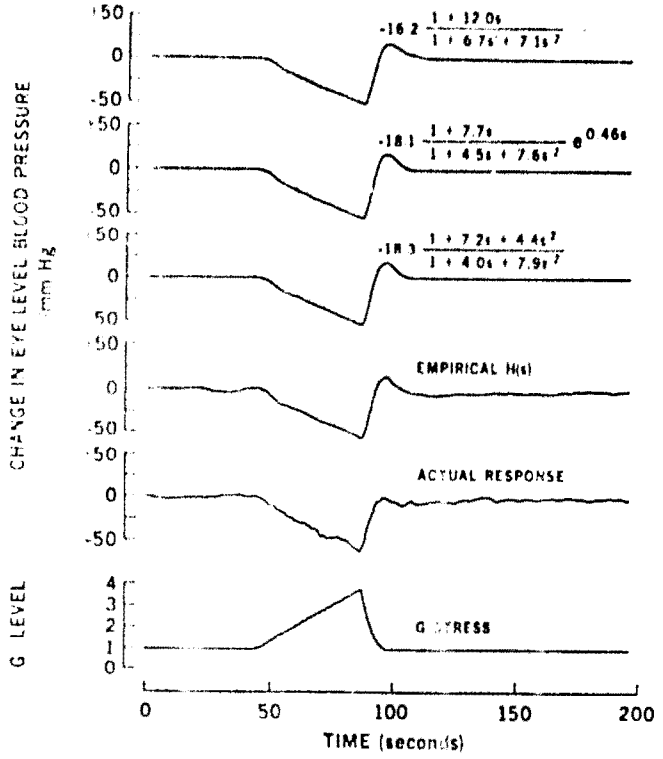

Fig. 8. Predicted and mean actual eye-level blood-pressure responses to GOR G stress. In this and the following figures, top trace is prediction based on single-zero, double-pole transfer function; second, single-zero, double-pole, exponential; third, double-zero, double-pole; fourth, 23-run mean empirical. Fifth trace is mean actual response of three subjects to G stress indicated in bottom trace.

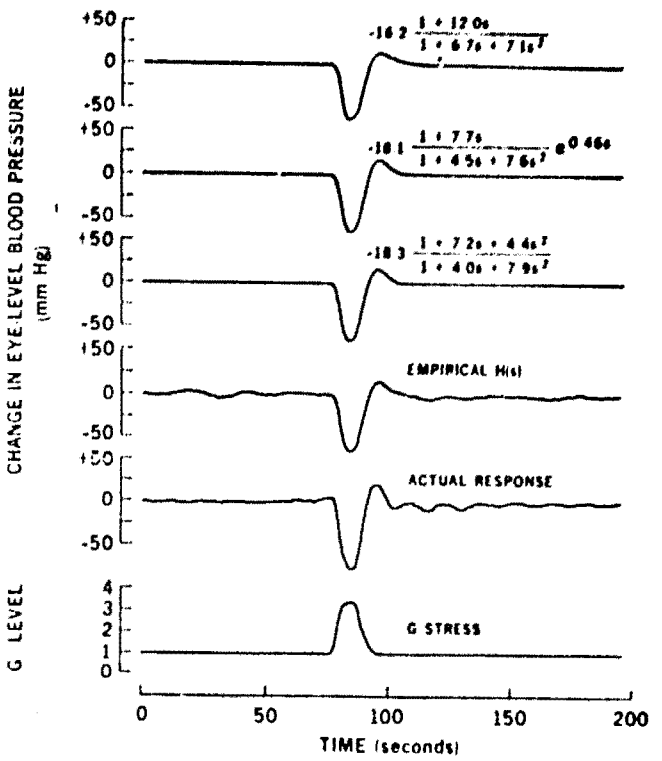

Fig. 9. Predicted and mean actual eye-level blood-pressue responses to aborted ROR G stress. Sequence as in Fig. 8.

responses to a variety of G-stress profiles. The predicted responses to a typical GOR G-stress profile (Fig. 8), although quite similar to each other in the amount of blood-pressure drop at peak G and amount of overshoot following deceleration, were disappointingly not very well matched to the mean actual response during the period of expected blood-pressure rebound. Fortunately, the reason for the discrepancy lies not with the transfer functions but with the subjects' mean response to the GOR G stress: only one response to this type of stress was obtained from each subject, and two of the three responses were decidedly atypical when compared with blood-pressure responses to GOR G stress obtained in this laboratory on other occasions.

More satisfactory was the comparison of the various predictions with the mean actual response to ROR G stress. Both the predicted and mean actual responses to an aborted ROR (Fig. 9), bearing understandable similarity to the impulse responses of the analytic transfer functions, displayed an initial blood-pressure drop proportional to G load and an overshoot occurring during and after deceleration. The prerun rise and the postrun oscillation in pressure seen in the mean actual response were not predicted by either the empirical or the analytic transfer functions. A particularly rigorous test of the predictive abilities of the various transfer functions was the 60-s ROR G profile (Fig. 10), since subtle differences in the responses were accentuated by

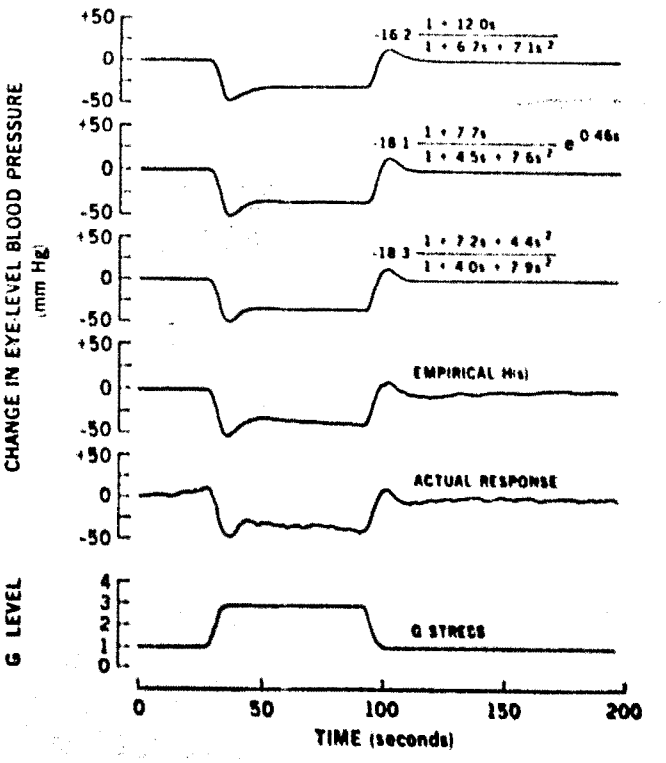

Fig. 10. Predicted and mean actual eye-level blood-pressure responses to 60-s ROR G stress. Sequence as in Fig. 8.

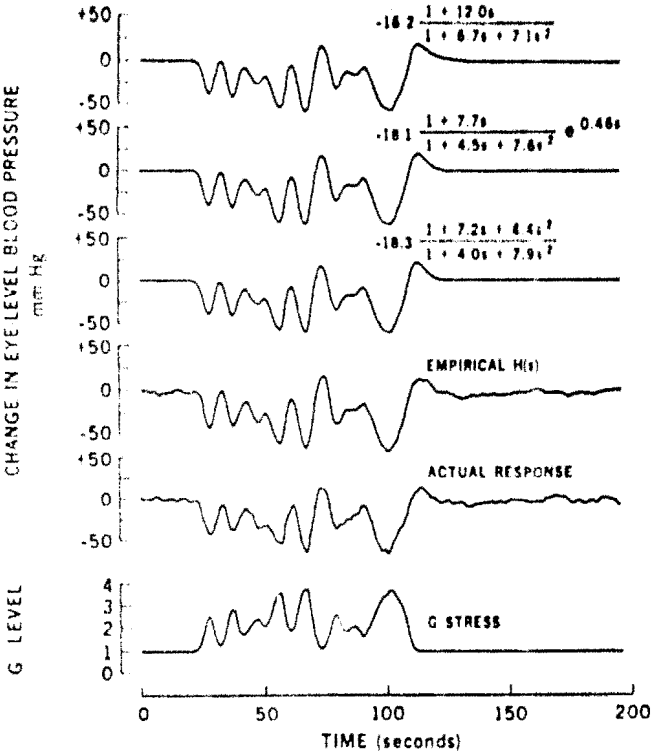

Fig. 11. Predicted and mean actual eye-level blood-pressure responses to #8 SACM G stress. Sequence as in Fig. 8. To avoid contaminating prediction with actual response data, data from each subject's #8 SACM run were subtracted from empirical transfer function prior to making prediction.

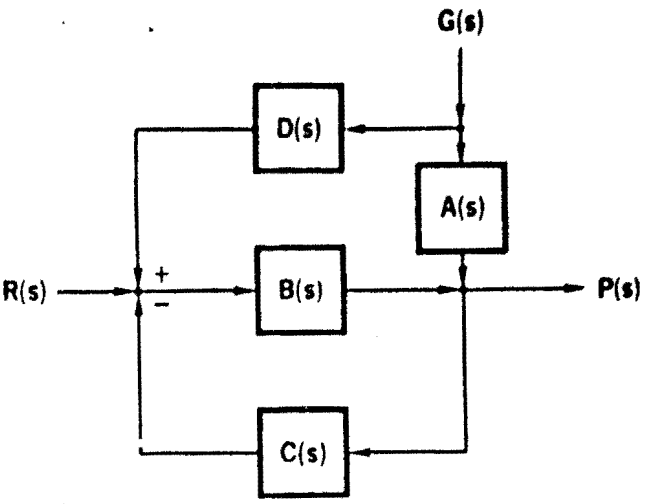

Fig. 12. Block diagram of eye-level blood-pressure control system for relaxed humans exposed to $+G_z$ stress. A(s), B(s), C(s), and D(s) are the hydraulic, neurocirculatory effector, baroceptor, and vestibulocerebellar components of the control system, respectively. R(s) is the reference signal, P(s) is eye-level blood pressure, and G(s) is G-stress perturbation.

the long, straight lines of the forcing function. The mean actual response to ROR G stress showed a number of characteristics coinciding with expectations based on prior experience: 1) an anticipatory rise in blood pressure prior to onset of G stress; 2) a rapid fall in pressure at onset of G stress; 3) a partial recovery of pressure several seconds after the G load had stabilized; 4) a secondary gradual decline in pressure following the peak of the partial recovery; 5) a rapid rise in pressure at the offset of G stress; 6) an overshoot in pressure coincident with termination of the G load; and 7) a small undershoot immediately following the terminal overshoot. Whereas the empirical and analytic transfer functions all predicted the pressure drop at onset, pressure rise at offset, partial recovery at stabilization, and overshoot at termination of G stress, they met with varying degrees of success in predicting other components of the waveform. Not one recreated the anticipatory rise in eye-level blood pressure. Only the empirical transfer function predicted the gradual decline in pressure during the constant G stress, and only the empirical provided a noticeable undershoot following the terminal overshoot. It is worthy of note that the predicted responses to ROR G stress had the same general characteristics as the classic figures presented by Wood and others (11,16); in fact, the greatest congruity with Wood's data was obtained with the empirical transfer function, in that it effectively reproduced the gradual decline in pressure during the latter portion of the plateau. Of the analytic transfer functions, both the double-zero and the exponential forms yielded more accurate predictions than did the single-zero form, which provided too smooth a transition into the partial recovery phase during G stress and too gradual a postrun return to mean pressure.

By averaging the individual transfer functions obtained from all SACM G-stress runs, except that SACM run for which a prediction is to be made, a mean transfer function uninfluenced by the test SACM can be obtained. Such transfer functions were used to make predictions of eye-level blood-pressure response to the several different forms of SACM G stress. Fig. 11 shows the mean actual response to the #8 SACM, as well as responses to this SACM predicted by the three analytic transfer functions and by the empirical transfer function with #8 SACM data excluded. Although it was difficult to evaluate visually the relative accuracy of predicted responses to so complex a waveform as the #8 SACM profile, such characteristics as the relative depths of the first two negative peaks, the relative heights of the highest two positive peaks, and the shape of the recovery from the terminal rebound enabled us to observe that the empirical transfer function was the most accurate.

To determine the goodness of fit of the three analytic transfer functions to the 23-run mean empirical transfer function, the standard error of estimate was obtained for each. This figure of merit was 4.02 for the single-zero, double-pole model; 3.34 for the single-zero, double-pole, exponential model; and 3.26 for the double-zero, double-pole model. The double-zero, double-pole transfer function thus emerged as the best of the analytic functions tested in that it most closely matched the empirical transfer function.

DISCUSSION

We recognize the limitations of using linear systems analysis techniques on notoriously nonlinear, nonstationary, biological systems. The blood-pressure control system was reasonably tractable to Fourier analysis, however, since well-behaved frequency response functions could be recognized and substantial predictive ability of derived transfer functions could be demonstrated. With regard to selection of the most appropriate transfer function, it appears that the first 40 terms of the empirical transfer function would be the logical choise if one requires greatest predictive accuracy and closest ties to experimental data. If concise mathematical expression is of greater importance, the double-zero, double-pole transfer function should be sufficient. Use of the single-zero, double-pole, exponential transfer function would not be justified since no advantage of the exponential term over an additional zero is demonstrable.

A simplified block diagram for the eye-level blood-pressure control system in relaxed humans exposed to G stress is shown in Fig. 12. The G-to-pressure transfer function, H(s), is thus described in this scheme as

$$H(s) = \frac{A(s) + B(s)D(s)}{1 + B(s)C(s)} \qquad \text{(Eq. 7)}$$

where A(s) represents the direct effects of the hydrostatic load on the blood and body, B(s) includes the various neural, hormonal, and mechanical effectors that translate control signals into blood pressure (primarily via changes in heart rate, venous compliance, and arterial resistance), and C(s) represents the dynamics of the several baroceptor feedback mechanisms. The effects of the vestibulocerebellar inputs to the cardiovascular control system are included in D(s). The hydrostatic column effect *per se* is frequency-independent, so that at very low frequencies of G stress, the hydrostatic column effect predominates; at higher frequencies, the frequency-dependent properties of compliant body structures, vestibulocerebellar pathways, cardiovascular effector mechanisms, and the baroceptor feedback loops become increasingly important. The properties of purely passive elements, i.e., the elasticity of the vascular tree and the inertia of the enclosed blood, provide a potential for resonance, which is the reason A(s) is denoted as a complex variable in the G-to-blood-pressure transfer function. The vestibulocerebellar effects on blood pressure are likely proportional-plus-derivative in form, since the vestibulocerebellar mechanisms appear to participate mainly in initiating, but also in sustaining, the orthostatic reflexes (1). This implies that D(s) in the G-to-blood-pressure transfer function is a term no simpler than $K_1(1 + K_2s)$. The open-loop transfer characteristics of the carotid sinus baroceptor system have been studied in animals (8,10,13), and the evidence indicates, at the very least, an integrating function of the form $K_3/(1 + K_4s)$, where the time constant K_4 is on the order of 20 or 30 s. The linear portion of one reported model (10) based on the input-output behavior of the canine carotid sinus reflex is of the form $K_3/(1 + K_4s + K_5s^2)$; interestingly, this double-pole model has a natural frequency of 42 mHz, which is not far from the resonance point of the empirical transfer function obtained in the present experiment. Another such model (13) even suggests a single-zero, double-pole loop transfer characteristic. From such evidence we should certainly expect that the combined transfer function, incorporating the elastic elements, the vestibulocerebellar pathway, and the baroceptor feedback loop, contains at least one zero and two or more poles. The evidence for additional zeros and poles at frequencies above 1.0 Hz (8) must be taken into account in the inevitable complete model of the blood-pressure control system, but is not particularly relevant to our discussion of blood-pressure responses to low-frequency G stress.

Knapp *et al.* (7) recently plotted the frequency response of the canine cardiovascular system as a whole. Using ± 2.0 G_z sinusoidal input stress at discrete frequencies from 0.001 to 1.5 Hz, they obtained the G-to-blood-pressure transfer characteristic; maximum gain was observed at 30 to 60 mHz, in rough agreement with our own data on the human response. They also reported that the frequency response of dogs with heart rate kept constant and peripheral vascular response blocked pharmacologically displayed a maximum between 40 and 60 mHz, confirming the complex form for the purely hydraulic segment of the blood-pressure control system. Also of interest were their observations that the influence of peripheral mechanisms was present up to 30 mHz, while heart-rate responses were most apparent in the 20- to 100-mHz range, thus providing additional evidence that the net G-to-blood-pressure transfer function consists of multiple poles and zeros.

Such data as are presented herein for relaxed humans and by Knapp *et al.* for dogs are the type prerequisite for the development of models like that of Green and Miller (5) and that of Witte *et al.* (15). We hope that those who develop models of cardiovascular function during G stress will decompose the overall transfer functions presented to obtain estimates of the transfer characteristics of the various segments of the blood-pressure control system. We also hope these data will be useful to modelers of pilot performance during aerial combat maneuvering. Required for such use, however, is a proper description of the changes in cardiovascular dynamics resulting from straining maneuvers and the use of anti-G suits, valves, and seats. Since straining maneuvers and the operation of most anti-G protective equipment are highly nonlinear, it would be necessary to model these effects separately, then add them to the basic blood-pressure control system, rather than to try to model as a linear system the overall mechanism of the protected cardiovascular response to G stress.

CONCLUSION

Data describing the eye-level blood-pressure response to $+G_z$ stress in relaxed humans have been presented as an empirical G-to-blood-pressure transfer function. This

transfer function covers the frequency spectrum from 5 to 200 mHz, and exhibits substantial predictive ability in the 1.0-4.5 G, 0-200 s ranges. Three simple mathematical models of the G-stressed blood-pressure control system were also tested for predictive ability, and were found moderately valid. Of these, the double-zero, double pole transfer function most closely fits the empirical transfer function, and appears to predict most accurately.

REFERENCES

1. Doba, N., and D. Reis. 1974. Role of the cerebellum and the vestibular apparatus in regulation of orthostatic reflexes in the cat. *Circulation Res.* 34:9-18.
2. Gauer, O. 1961. The hydrostatic pressures. *In:* O. Gauer and G. Zuidema (Eds.), *Gravitational Stress in Aerospace Medicine.* Little, Brown and Co., Boston.
3. Gauer, O., and E. Salzman. 1961. Reflex responses of the circulation. *In:* O. Gauer and G. Zuidema (Eds.), *Gravitational Stress in Aerospace Medicine.* Little, Brown and Co., Boston.
4. Gillingham, K., and R. Burton. 1975. Transfer functions for arterial oxygen saturation during $+G_z$ stress. *Aviat. Space Environ. Med.* 46:1329-1335.
5. Green, J., and M. Miller. 1973. A model describing the response of the circulatory system to acceleration stress. *Ann. Biomed. Engineering* 1:455-467.
6. Kirchheim, H. 1976. Systemic arterial baroreceptor reflexes. *Physiol. Rev.* 56:100-176.
7. Knapp, C., D. Randall, J. Evans, and J. Marquis. 1976. Frequency response of cardiovascular regulation in canines to sinusoidal acceleration at frequencies below 1.5 Hz. Presented at Review of Air Force Sponsored Basic Research in Environmental and Acceleration Physiology. Wright-Patterson AFB, Oh, 13-15 October.
8. Koushanpour, E., and J. Spickler. 1975. Effect of mean pressure levels on the dynamic response characteristics of the carotid sinus baroceptor process in dog. *IEEE Trans. Biomed. Engineering* BME-22:502-507.
9. Lawton, R., L. Green, G. Kydd, L. Peterson, and R. Crosbie. 1958. Arterial blood pressure responses to G forces in the monkey: I. Sinusoidal positive G. *J. Aviat. Med.* 29:97-105.
10. Levison, W., G. Barnett, and W. Jackson. 1966. Nonlinear analysis of the baroreceptor reflex system. *Circulation Res.* 18:673-682.
11. Lindberg, E., and E. Wood. 1963. Acceleration. *In:* J. Brown (Ed.), *Physiology of Man in Space.* Academic Press, New York.
12. Rogers, D. 1975. An acceleration stress endpoint model for combat maneuvering analysis. Preprints of scientific program, Aerospace Medical Association, pp. 273-275.
13. Scher, A., and A. Young. 1963. Servoanalysis of carotid sinus reflex effects on peripheral resistance. *Circulation Res.* 12:152-162.
14. Spickler, J., and P. Kezdi. 1967. Dynamic response characteristics of carotid sinus baroreceptors. *Amer. J. Physiol.* 212:472-476.
15. Witte, E., A. Phatak, and J. Green. 1975. Evaluation of physiological inputs to high-G performance models. AMRL-TR-74-103, Aerospace Medical Research Laboratory, Wright-Patterson AFB, Oh.
16. Wood, E., and E. Lambert. 1952. Some factors which influence the protection afforded by pneumatic anti-G suits. *J. Aviat. Med.* 23:218-228.